Talanta Open 4 (2021) 100048

Contents lists available at ScienceDirect

Talanta Open

journal homepage: www.sciencedirect.com/journal/talanta-open

Polymer substrate with surface solvent reservoir for polymer-spray mass spectrometric analysis of hydrophilic drugs

Maria T. Dulay [a], Cornelia L. Boeser [b], Katherine L. Walker [b], Clara Feider [b], Richard N. Zare [a,*]

[a] Department of Chemistry, Stanford University, Stanford, CA, 94305, USA
[b] Thermo Fisher Scientific, San Jose, CA, 95134, USA

ARTICLE INFO

Keywords:
Polymer spray mass spectrometry
Surface solvent reservoir
Hydrophilic drugs

ABSTRACT

Nonporous, hydrophobic organosiloxane (OSX) polymers with surface reservoirs were developed as sampling supports in polymer-spray mass spectrometry (polyS-MS) for the detection and quantification of hydrophilic drugs, ethyl glucuronide (logP -1.8) and vancomycin (logP -4.4), and a slightly hydrophobic drug, phenobarbital (logP 1.5). OSX polymers with surface reservoirs were prepared by solvent evaporation-induced patterning in the presence of an ionic liquid during sol-gel polymerization of a methylalkoxysilane. The surface reservoir provides a continuous supply of spray solvent, enhancing both signal stability and signal duration when conducting analysis by polyS-MS. Using OSX polymer substrates with surfaces reservoirs, calibration curves were generated with good linearity (R^2>0.99) and reproducibility and low data spread over the concentration ranges used to screen each of the drugs tested as compared to paper substrates: ethyl glucuronide, 5 – 1000 ng/mL (methanol) and 50 – 10,000 ng/mL (synthetic urine); vancomycin, 2 – 100 μL/mL (plasma); phenobarbital, 50 – 50,000 ng/mL (methanol) and 50 – 5000 ng/mL (synthetic urine). Quantitative analysis by polyS-MS of phenobarbital samples in synthetic urine at concentrations of 250 ng/mL and 2,500 ng/mL showed good recoveries of 90.2% (RSD 3.51%) and 95.7% (RSD 2.57%), respectively. Compared to paper substrates, OSX polymers gave calibration curves with better linearity and reproducibility, especially at low concentrations, as well as longer signal durations, improved signal stabilities, and increased signal intensities. Little to no sample pretreatment is necessary and the required sample volume is small (1 μL to 2 μL), making polyS-MS easy to use for high throughput sample processing.

1. Introduction

Therapeutic drug monitoring (TDM) has become a critical tool in disease management for the determination of appropriate drug concentrations, resulting in better drug efficacy and reduced toxicity [1], and in treatment of drug abuse [2]. Common methodologies for TDM include immunoassays and chromatographic techniques that are often coupled to mass spectrometry, which can achieve much higher degrees of specificity than immunoassays [3,4]. In recent years, paper-spray mass spectrometry (PS-MS), a form of ambient ionization mass spectrometry, has emerged as a rapid, robust quantitative and qualitative alternative for the analysis of therapeutic drugs with little to no sample preparation required [5–13]. However, hydrophilic drugs are not as easily detected or quantified using standard filter paper and in some cases the drug is not detected at all [13]. Hydrophobic paper [14–18], including silica-coated [20,21], wax-coated [19,22], and polymer-coated [23–26] modifications, has been explored as an alternative to the traditional hydrophilic cellulosic paper substrate to reduce the affinity of a hydrophilic analyte to the paper surface.

Recently, we reported on the use of hydrophobic polymer sample supports in polymer-spray mass spectrometry (polyS-MS) for the detection of hydrophilic drugs, such as streptomycin, that are not easily detected using PS-MS [13]. The nonporous organosiloxane (OSX) polymers that replaced the porous cellulosic paper substrates overcame some of the drawbacks of paper, namely, less background interference and decreased affinity to or trapping of analytes. In addition, OSX polymers can be cleaned without compromising their structural integrity, and we have observed no analyte carryover during their reuse.

One of the unique features of the OSX polymer is the ability to control the reaction conditions to afford polymers with different morphologies or different surface chemistries. By controlling solvent evaporation and phase separation that are part of sol-gel polymerization,

* Corresponding author.
E-mail address: rnz@stanford.edu (R.N. Zare).

https://doi.org/10.1016/j.talo.2021.100048
Received 4 April 2021; Received in revised form 31 May 2021; Accepted 1 June 2021
Available online 9 June 2021

Table 1
Dimensions of individual triangles molds formed in a PDMS mold.

Triangle	*Height* (cm)	*Base* (cm)	*Side* (cm)	*Depth* (mm)
A	1.46	1.3	1.6	2
B	1.52	1.1	1.6	1
C	1.55	0.8	1.6	0.5

reservoirs were created on the surface of OSX polymers to hold adequate volumes of spray solvent. Maintaining a steady volume of spray solvent during a PS-MS analysis is critical in establishing stable electrospray ionization and recording analyte signals for longer than the typical 1-minute period [20]. Various approaches have been implemented to maintain continuous spray, such as the use of excess spray solvent [27] or connecting a paper substrate to an external solvent reservoir [28,29].

In our present study, we compare paper, flat OSX polymers, and OSX polymers with a solvent reservoir formed at the surface as substrates for the analysis of compounds in complex media. A solvent reservoir is formed at the surface of an OSX polymer by (1) controlling solvent evaporation to afford evaporation-induced patterning [30] and (2) by incorporating a room-temperature ionic liquid to control phase separation [31] of the alkoxysilane oligomers during polymerization in a triangular mold. This approach is similar to the formation of a coffee ring [32]. The reservoir on the OSX polymer surface localizes and contains the solvent which reduces the spread of the spray solvent on the polymer surface and minimizes the loss of spray solvent through evaporation. Enhancements in signal intensity and improved signal duration afforded increased analysis time adequate to complete monitoring of fragmentation in tandem MS experiments. A nonporous polymer with a surface reservoir offers additional advantages, including (1) separation of the deposited sample and solvent to reduce dilution of analytes, (2) rapid and easy alignment of the polymer substrate with a mass spectrometer inlet for high throughput analysis (as compared to a flat-surface polymer), (3) reusability of the polymers by simple cleaning with appropriate solvent so there is no carryover from previous use, and (4) reproducible fabrication (same triangle size and reservoir depth). We use OSX polymers with surface reservoirs as sampling supports in polyS-MS for the detection and quantitation of hydrophilic drugs, ethyl glucuronide (logP -1.8) [33] and vancomycin (logP -4.4) [33], and a slightly hydrophobic drug, phenobarbital (logP 1.5) [33], which are not easily detectable by PS-MS. The presence of a surface reservoir is an added improvement in quantitation and ease of use over that of a flat-surface OSX polymer [13].

2. Experimental section

2.1. Chemical and materials

1-Butyl-3-methylimidazolium tetrafluoroborate ($[BMIM]^+[BF_4]^-$), 1-butyl-3-methylimidazolium pentahexafluoride ($[BMIM]^+[PF_6]^-$), methyltrimethoxysilane and vancomycin were purchased from Sigma-Aldrich (Milwaukee, WI, USA) and used without further purification. Ethyl glucuronide, ethylglucuronide-d5, phenobarbital, and phenobarbital-d5 were purchased from Cerilliant (Round Rock, TX, USA). Vancomycin-d12 trifluoroacetate salt (95% enriched) was purchased from AlsaChim (Illkirch-Graffenstaden, France). Human plasma K2EDTA was purchased from BioIVT (Medford, MA, USA) and synthetic urine (*S*urine) from DTI (Lenexa, KS, USA). Optima, HPLC, or UHPLC quality methanol, isopropyl alcohol, dichloromethane, tetrahydrofuran, acetonitrile, water, ammonium hydroxide and acetic acid were purchased from Thermo Fisher Scientific (Waltham, MA, USA) and used without further purification. Momentive RTV615 Clear 010 potting compound and RTV615 crosslinking agent for the preparation of PDMS positive mold was purchased from Newark Co. (Chicago, IL, USA).

2.2. Preparation of substrate mold

A 3D-printed reverse mold made of polycarbonate consisted of three different isosceles triangles with varied dimensions and depths as listed in Table 1 and shown in Fig. 1A. The positive mold was prepared with PDMS polymer by mixing 10:1 (*w/w*) RTV615 Clear 010 potting compound to crosslinking agent, and then degassing to remove all trapped air bubbles before pouring into the polycarbonate reverse mold. Curing of the polymer was achieved overnight (20-24 h) at room temperature, resulting in a clear, colorless PDMS positive mold (Fig. 1B) with flexibility that allows easy removal of the OSX polymer triangles after polymerization (Fig. 1C).

2.3. Synthesis of OSX Polymer

A room-temperature ionic liquid (RTIL) solution of 54 mM $[BMIM]^+[BF_4]^-$ or $[BMIM]^+[PF_6]^-$ was prepared in 0.12N HCl. In a 20-mL glass vial, 1.8 mL of 54 mM RTIL/HCl solution was added dropwise to 7.8 mL MTMS with stirring. The reaction solution was stirred at room temperature for 2.5 h with the glass cap loosely screwed on as the reaction is exothermic.

The PDMS positive mold was cut into sections containing the same dimension triangles to fit into a large Petri dish. Each of the triangle

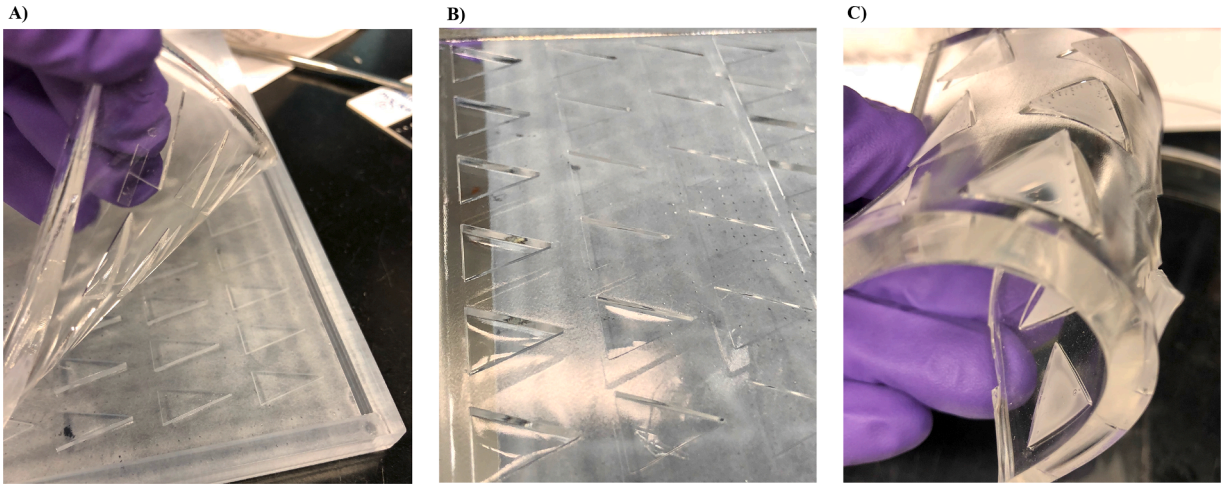

Fig. 1. (A) A flexible PDMS positive mold being peeled off a 3D-printed reverse mold, (B) clear, colorless PDMS positive mold with rows of triangle molds, and (C) removal of OSX polymers from the triangle molds by bending the PDMS mold.

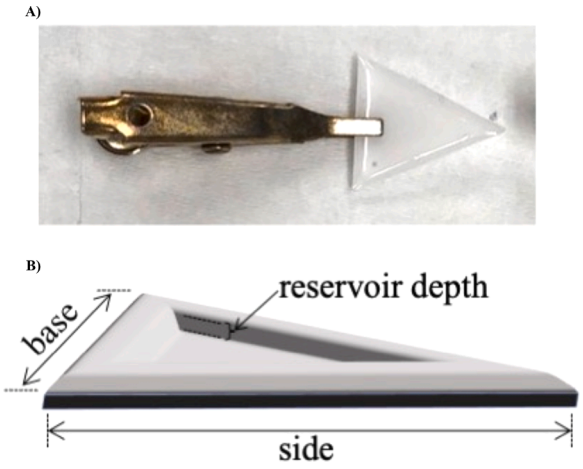

Fig. 2. (A) Photo of an OSX polymer with a surface reservoir; a flat alligator clip is attached to the polymer and (B) diagram showing geometry of a polymer.

molds were fully filled with the OSX reaction solution (75 µL to 200 µL, depending on the triangle size and depth). OSX polymerization proceeded for 24 h at room temperature and in a closed environment to prevent fast evaporation of water and the alcohol byproduct formed during the reaction. After polymerization, the rigid, opaque OSX triangles were removed from the flexible PDMS positive mold by gently bending it. The OSX triangles were submerged in 1:1 (*v*/*v*) acetonitrile: water and sonicated in a water bath for 10 minutes. After drying, the cleaned OSX triangles were stored at room temperature in a covered Petri dish until use. The final OSX triangles are presented in Fig. 2.

2.4. Drug calibration and quality control solutions

A calibration curve for each drug was created by preparing calibration solutions via serial dilution of working solutions. For polyS-MS experiments with phenobarbital (PB) in methanol, six working solutions were prepared with the following concentrations: 255 µg/mL, 102 µg/mL, 51 µg/mL, 25.5 µg/mL, 5.1 µg/mL, and 2.55 µg/mL PB. To prepare calibration solutions, 20 µL of a working solution and 5 µL of phenobarbital-d5 (PB-d5) internal standard (408 µg/mL) were added to 1 mL methanol to generate six solutions with concentrations of 5000 ng/mL, 2000 ng/mL, 1000 ng/mL, 500 ng/mL, 100 ng/mL, and 50 ng/mL PB. Each calibration solution contained 2000 ng/mL PB-d5. For PS-MS experiments, PB working solutions in methanol were prepared with the following concentrations: 125 µg/mL, 50 µg/mL, 25 µg/mL, 12.5 µg/mL, 2.5 µg/mL, and 1.25 µg/mL PB. To prepare the calibration solutions, a volume of 20 µL of a working solution and 10 µL of PB-d5 (100 µg/mL) were spiked into 470 µL methanol to generate six calibration solutions with concentrations of 5000 ng/mL, 2000 ng/mL, 1000 ng/mL, 500 ng/mL, 100 ng/mL, and 50 ng/mL PB. Each calibration solution contained 2000 ng/mL PB-d5.

For polyS-MS experiments with PB in *S*urine, PB working solutions in methanol were prepared at the following concentrations: 125 µg/mL, 50 µg/mL, 25 µg/mL, 12.5 µg/mL, 2.5 µg/mL, and 1.25 µg/mL. Six calibration solutions were prepared by adding 20 µL of a working solution and 10 µL PB-d5 (100 µg/mL) internal standard into 470 µL *S*urine to generate the following concentrations: 5000 ng/mL, 2000 ng/mL, 1000 ng/mL, 500 ng/mL, 100 ng/mL, and 50 ng/mL PB. Each calibration solution contained 2000 ng/mL PB-d5. For PS-MS experiments of PB in *S*urine, PB working solutions in methanol were prepared at the following concentrations: 125 µg/mL, 50 µg/mL, 25 µg/mL, 12.5 µg/mL, 2.5 µg/mL, and 1.25 µg/mL. Six calibration solutions were prepared by mixing 20 µL of a working solution and 10 µL PB-d5 (100 µg/mL) into 470 µL *S*urine to generate the following concentrations: 5000 ng/mL, 2000 ng/mL, 1000 ng/mL, 500 ng/mL, 100 ng/mL, and 50 ng/mL PB. Each calibration solution contained 2000 ng/mL PB-d5.

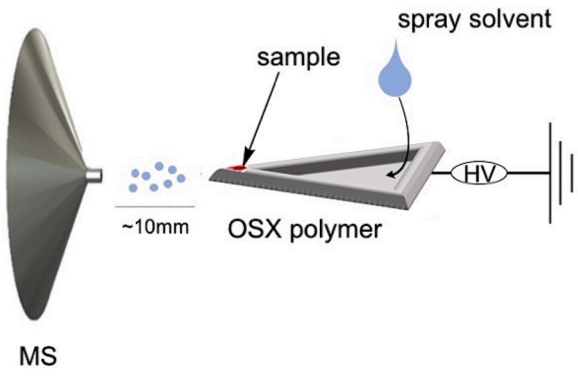

Scheme 1. (A) Diagram of polyS-MS.

For both polyS-MS and PS-MS experiments of ethyl glucuronide (EtG) in methanol, working solutions in methanol were prepared with the following concentrations: 25 µg/mL, 12.5 µg/mL, 2.5 µg/mL, 1.25 µg/mL, 0.51 µg/mL, and 0.25 µg/mL. Six calibration solutions were prepared by adding 20 µL of a working solution and 5 µL ethyl glucuronide-d5 (EtG-d5) internal standard (50 µg/mL) to 475 µL methanol to generate the following concentrations: 1000 ng/mL, 500 ng/mL, 100 ng/mL, 50 ng/mL 10 ng/mL, and 5 ng/mL EtG. Each calibration solution contained 500 ng/mL EtG-d5.

For both polyS-MS and PS-MS experiments with EtG in *S*urine, working solutions in methanol were prepared with the following concentrations: 250 µg/mL, 125 µg/mL, 25 µg/mL, 12.5 µg/mL, 2.5 µg/mL, and 1.25 µg/mL EtG. Six calibration solutions were prepared by adding 20 µL of a working solution and 10 µL EtG-d5 (50 µg/mL) internal standard into 470 µL *S*urine to generate the following concentrations: 10,000 ng/mL, 5000 ng/mL, 1000 ng/mL, 500 ng/mL, 100 ng/mL, and 50 ng/mL EtG. Each solution contained 1000 ng/mL EtG-d5.

For both polyS-MS and PS-MS experiments with vancomycin (VAN) in plasma, working solutions in 1:1 (*v*/v) methanol:water with 0.1% acetic acid were prepared with the following concentrations: 2.5 mg/mL 1.25 mg/mL, 0.5 mg/mL, 0.25 mg/mL, 0.125 mg/mL, and 0.05 mg/mL. Six calibration solutions were prepared by adding 20 µL of a working solution and 10 µL vancomycin-d12 (VAN-d12) internal standard (1 mg/mL) to 470 µL plasma to generate the following concentrations: 100 µg/mL, 50 µg/mL, 20 µg/mL, 10 µg/mL, 5 µg/mL, and 2 µg/mL VAN. Each solution contained 20 µg/mL VAN-d12.

Two quality-control (QC) PB solutions in *S*urine were prepared by diluting 6.25 µg/mL and 62.5 µg/mL PB working solution. A volume of 20 µL of working solution was added to 10 µL of 100 µg/mL PB-d5 in methanol and 470 µL *S*urine. The final concentrations of the QC PB solutions were 250 ng/mL and 2,500 ng/mL.

2.5. polyS-MS workflow

Scheme 1 shows a diagram of the polyS-MS set up. For each run, an OSX triangular surface-reservoir sample support was held with a flat alligator clip attached to the MS instrument's high-voltage power supply. The tip of the triangular sample support was aligned to the inlet of the mass spectrometer and positioned about 5-10 mm distance from the instrument inlet. The TSQ Endura mass spectrometer (Thermo Fisher Scientific) was used for PB in methanol polyS-MS experiments. The TSQ Quantis mass spectrometer (Thermo Fisher Scientific) was used for the remaining experiments. The runs for PB and EtG were performed in negative polarity mode while the runs for VAN were performed in positive polarity mode. Tandem mass spectrometry (MS/MS) of each drug for structural confirmation through collision-induced dissociation with 2 mTorr argon collision gas was performed with the following parent ions: PB molecular ion *m/z* 231.162 ($[PB\text{-}H]^-$), EtG molecular ion *m/z* 221.088 ($[EtG\text{-}H]^-$), and VAN molecular ion *m/z* 735.7 ([VAN-

Table 2
Spray solvents and high voltage used in each analysis.

Drug sample	*Analysis method*	*Spray solvent*	*Applied HV* (kV)
PB in MeOH	polyS-MS or PS-MS	80:20 (*v/v*) MeOH:CH_2Cl_2	3.1
PB in *S*urine	polyS-MS	80:20 (*v/v*) MeOH:CH_2Cl_2 + 80 ppm NH_4OH	3.1
PB in *S*urine	PS-MS	80:20(*v/v*) MeOH:IPA	3.1
EtG in *S*urine	polyS-MS or PS-MS	60:40 (*v/v*) MeOH:THF	3.5
VAN in plasma	polyS-MS or PS-MS	50:50 (*v/v*) MeOH:H_2O + 0.1% acetic acid	3.5

$HNa]^{2+}$). The ion transfer tube was heated to 300 °C for runs involving PB and EtG while the temperature was set at 325 °C for VAN runs. The acquisition parameters used are shown in Tables S1 to S5. Data were acquired and analyzed using Thermo Fisher QualBrowser software. The integration of sample signals (all transitions) and the corresponding internal standard were performed over 0.5 min.

For each set of polyS-MS runs, 1.5 μL of calibration solution was spotted at the tip of the polymer outside the surface reservoir and allowed to dry. Prior to a run, an initial volume of 40 μL of spray solvent was added into the reservoir on an OSX polymer. More spray solvent was added, if needed. Similarly, for PS-MS runs, 1.5 μL of calibration solution was spotted at the tip of a paper triangle substrate and allowed to dry. A volume of 40 μL or more of spray solvent was used to establish a stable signal. Each of the calibration solutions were run in triplicate.

For the quality control (QC) experiments with PB in *S*urine, 1.5 μL of QC solution was spotted as described for polyS-MS and PS-MS runs. Recovered PB was determined by using established calibration curves for PB in *S*urine.

Table 2 lists the spray solvents utilized in each experiment; the solvent was optimized for each condition. The run voltage applied to each OSX polymer ranged between 3.0 and 3.5 kV (Table 2) to generate a steady electrospray and introduce ions into the mass spectrometer. Please note that it is necessary to apply a voltage to achieve spray; with no voltage, no signal is observed. Three replicate runs were conducted for each calibration and QC solution concentration.

After use, each OSX polymer was cleaned by sonication in 1:1 (*v/v*) acetonitrile:water for 10 min. The polymer triangles were allowed to dry ambiently before storing in a Petri dish at room temperature.

3. Results and discussion

3.1. OSX polymer with surface reservoir

The reservoir on the polymer surface prevents spreading of the spray solvent across the polymer, minimizes solvent evaporation during an analysis, and allows for constant solvent flow to the polymer triangle tip. As a consequence, signal stability is enhanced, data acquisition time is increased, and alignment of the polymer tip with the MS instrument interface is simplified. Improved performance of PS-MS has also been reported with a configuration that provides constant solvent flow to the paper tip with an external solvent supply device [34] or a 3D-printed cartridge that serves as holder for the paper substrate and a dedicated solvent reservoir [35].

OSX polymers with surface reservoirs were prepared by sol-gel chemistry with methyltrimethoxysilane (MTMS), which has been used previously to prepare flat-surface OSX polymers used for polyS-MS [13]. In the presence of a room-temperature ionic liquid (RTIL) the morphology of the resulting polymer can be modified. The high ionic strengths of RTILs increase the aggregation rate of the sol-gel reaction, allowing hydrolysis and condensation to proceed to completion and produce a stable polymeric network [36]. RTILs have typically been used (1) to promote self-assembly of the OSX oligomers formed during the polymerization in water and (2) to minimize mesopore collapse during post-reaction workup that would lead to cracks in the resulting polymer. Two RTILs were tested: hydrophilic $[BMIM]^+[BF_4]^-$ and hydrophobic $[BMIM]^+[PF_6]^-$. The type of anion did not appear to have a significant effect on the polymerization time of MTMS in dilute acid although it has been reported that RTILs with $[BF_4]^-$ anion highly promotes the hydrolytic condensation of alkoxysilanes with higher catalytic activity than RTILs with $[PF_6]^-$ anion [37]. In the presence of $[BMIM]^+[PF_6]^-$, the reaction solution was homogeneous during the 2.5-h pre-polymerization stirring period at room temperature. A mechanically robust, opaque OSX polymer was produced by casting the reaction solution in a mold at room temperature for 24 hours. It has been reported that $[BF_4]^-$ anion promotes strong H-bonding between the RTIL and the sol-gel oligomers, resulting in mechanically stable polymers [38]. However, the polymer resulting from the reaction solution containing $[BMIM]^+[BF_4]^-$ was thinner and easily broken. At a H_2O/Si ratio of 3.7, there is sufficient water in the reaction mixture to afford hydrolysis of nearly all the alkoxy groups of MTMS into silanol groups regardless of the RTIL.

Over the last 10 years, "template-controlled" evaporation patterning has been developed to fabricate well-ordered surface structures similar to a "coffee ring," which is the typical self-organized pattern induced by the evaporation of solvent [39,40]. In recent years, non-templated patterning involving phase separation by solvent evaporation [30,41] or application of an electric field [40], has been shown to promote symmetric patterns on polymer surfaces. Polymeric structures with walls have been created by exploiting phase separation during polymerization [42]. Phase separation plays a role in sol-gel reactions to produce well-defined heterogeneous structures [43], but it does not typically promote the formation of a pattern on the bulk polymer surface.

When an OSX polymer is cast in a triangle-shaped mold, the edges of the triangular polymer are raised compared to the rest of the polymer surface, resulting in a distinct triangular surface reservoir and a raised triangular tip where sample can be deposited. This structure is due to solvent evaporation and phase separation. Liquid evaporating from the edge of a solution is more significant than evaporation at the center of the solution; therefore there is radially outward Marangoni flow that brings the solute to the perimeter in order to balance the local mass, resulting in increased concentration at this edge while the concentration gradually decreases at the center of the solution [44]. If the evaporation-driven flow proceeds much more quickly than local mass balancing by diffusion, then dissolved oligomers/polymer are deposited primarily at the periphery of the drop [45]. The result is the development of a marked rim at the periphery of the evaporating solution similar to the "coffee ring" effect. Geometrical characteristics of the "coffee-ring" patterns are dependent on the shape of the templates or mold [45].

The presence of an ionic liquid, which acts to induce self-assembly of the OSX oligomer precursors during the early stages of the polymerization, likely influences the surface tension of the solution. Unique highly ordered patterns have been created under the influence of surface tension when a surfactant is present [46]. Solvation of water molecules within the bulk of hydrophilic $[BMIM]^+$ $[BF_4]^-$ is promoted by favorable molecular interactions, including H-bonding, while it has been shown that hydrophobic $[BMIM]^+[PF_6]^-$ is more sensitive to the presence of water, resulting in the reorientation of $[BMIM]^+$ forcing water molecules to the surface of the gas-liquid interface to better solvate them, resulting in vastly different morphologies [47]. These features may influence solvent evaporation during polymerization and play a role in the formation of a surface reservoir on the resulting OSX polymer.

It might be questioned whether the substrates for polymer spray reported here are robust and whether the process can be readily scaled. Although we did not systematically test their long-term stability, the OSX polymers used in the study were at least two years old and stored under ambient conditions. Even after two years, these OSX polymers showed good reproducibility. Scalability can be addressed by preparing

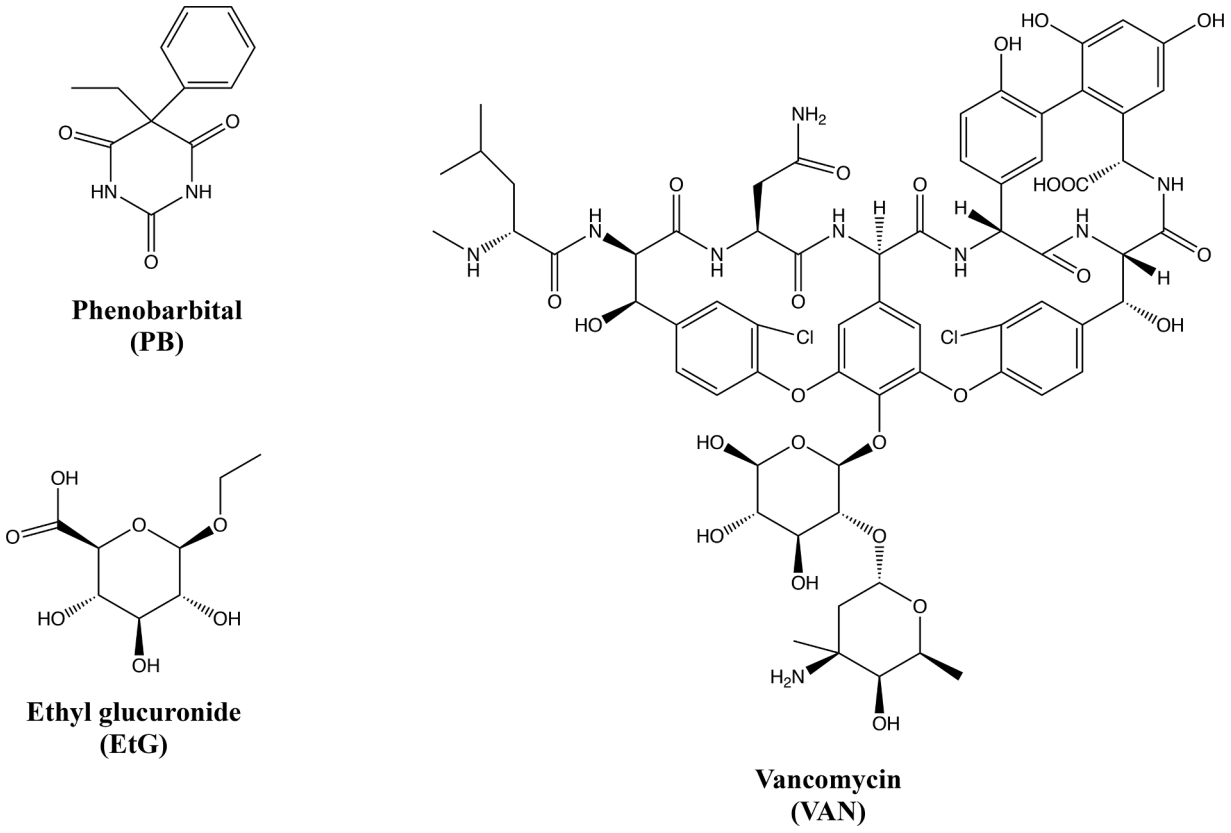

Scheme 2. Structures of drug analytes.

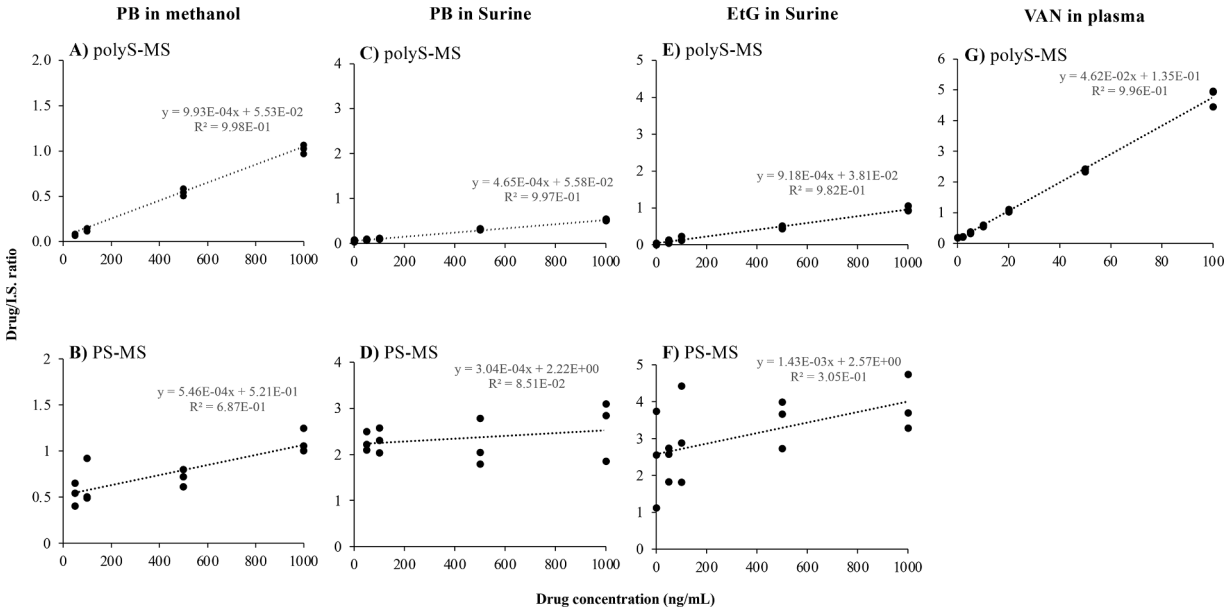

Fig. 3. Calibration curves at the lower end of the concentration ranges for phenobarbital (PB) in methanol (**A, B**), PB in Surine (**C, D**); ethyl glucuronide (EtG) in Surine (**E, F**) and vancomycin (VAN) in human plasma (**G**) analyzed by polyS-MS and PS-MS.

a mold with many more triangle templates from which the OSX polymers can be fabricated. The alternative is to prepare these OSX polymers by 3D printing

3.2. Drug calibration curves by polyS-MS and PS-MS

In this study, three drugs with different polarities (Scheme 2) were analyzed by polyS-MS, using OSX polymers with surface reservoirs, and calibration curves were generated and compared to calibration curves from PS-MS experiments, using VeriSpray paper from Thermo Fisher Scientific. The hydrophilicities of these drugs are described by their logP values, where logP is the partition coefficient of the concentration of the compound in octanol compared to being in water [33]. Fig. 3 shows the calibration curves at the lower concentration range. When analyzed by

Table 3
Linear regression (R^2) data from calibration curves for PB, EtG, and VAN using OSX polymer with surface reservoir for polyS-MS and VeriSpray paper (Thermo Fisher Scientific).

Drug	*R^2, polyS-MS*	*R^2, PS-MS*	*Sample matrix*	*logP*
PB	0.998	0.974	MeOH	1.47
PB	0.998	0.484	*S*urine	1.47
EtG	0.996	0.886	*S*urine	-1.8
VAN	0.996	n.d.	human plasma	-4.4
VAN (flat polymer)	0.973	n.d.	human plasma	-4.4

polyS-MS, the calibration curves for each drug in solvent or a complex matrix showed good linearities (R^2>0.99) with very little spreading of data at the lower end of the concentration range (≤1000 ng/mL). When analyzed by PS-MS, PB in methanol, PB in *S*urine, and EtG in *S*urine by PS-MS had calibration curves with poor linearities and significant spreading of data. Table 3 presents a summary of the calibration curve linearities. Please note that each point in a calibration curve represents three replicate measurements. For each replicate, a different OSX polymer was used. Thus, these OSX polymers, which came from three different batches, demonstrated high reproducibility.

Nonporous, hydrophobic OSX polymer has been shown to be a good alternative to paper, providing a cleaner MS background and improved signal stability [13]. It has been reported that the thickness and porosity of paper used in PS-MS affects ionization efficiency. Smaller pores in paper contribute to increased ionization efficiencies [5]. In the negative polarity mode, hydrophobic sample substrates have improved signal as compared to paper sample supports.

To test the utility of polyS-MS as a quantitative technique, two different quality control samples of PB in *S*urine were analyzed using OSX polymers with surface reservoirs to quantify PB. These OSX polymers with surface reservoirs were simpler to align with the mass spectrometer interface as compared to the same polymer with flat surfaces, allowing for higher throughput. And the OSX polymers were easy to clean, making them reusable without any carryover of analytes from previous experiments.

Phenobarbital in methanol. Phenobarbital (PB), a slightly hydrophobic drug (logP 1.47), is a barbiturate with anticonvulsant properties. Its minimum clinical toxic level is 30 μg/mL.

The calibration curves were generated by plotting PB in methanol calibration solution concentrations (50-5000 ng/mL) vs PB:PB-d5 area ratios from polyS-MS data and PS-MS data (Table 3). The polyS-MS calibration curve from OSX polymer with a surface reservoir exhibits good linearity (R^2 = 0.998) over the analyzed concentration range. Good linearity (R^2 = 0.998) was also achieved when an OSX polymer with a flat surface was used (Figure S1). Poorer linearity (R^2 = 0.974) was achieved using PS-MS. Fig. 3A and B show the calibration curves at the lower concentration range from 50 ng/mL to 1000 ng/mL for polyS-MS and PS-MS, respectively. When a paper substrate is used for the analysis of PB in methanol, there is a larger spread of the replicates as compared to the OSX polymer. This deviation contributes to the poor linearity of the calibration curve. Furthermore, the positive y-intercept falls at 0.5, as shown in Fig. 3B, because of high background signal when using paper, which can often contain contaminants. OSX polymers, which can be easily cleaned, have little to no background signals that interfere with analysis (Figure S2) [13]. For both polyS-MS and PS-MS, the parent ion (*m/z* 231) was fragmented using a range of collision energies to afford several product ions, including the corresponding $[M\text{-}H]^-$ product ion (Tables S1 and S2, respectively). The parent ion of PB-d5 has an *m/z* 236.2.

Phenobarbital in Surine. Calibration curves for PB in *S*urine obtained by polyS-MS has good linearity (R^2 = 0.997) that is comparable to the linearity (R^2 = 0.998) obtained for PB in methanol by polyS-MS (Table 3). Similarly, the background signal was low with a near-zero y-intercept, as shown in Fig. 3C. In contrast, the linearity of the calibration curve using a paper sample support was very poor (R^2 = 0.484, Table 3). The area ratios at each calibration curve concentration for PB obtained by PS-MS did not show good reproducibility, resulting in a large spread of the replicates between 50 ng/mL and 1000 ng/mL as shown in Fig. 3D. The value of the y-intercept in the PS-MS calibration curve is high at about 2.1 because of the high background signal from contaminants in the paper and *S*urine. Fragmentation of the *m/z* 231 parent ion in both polyS-MS and PS-MS experiments yielded similar fragment ions (Table S3) as for PB in methanol samples.

Ethyl glucuronide (EtG) in Surine. EtG is one of the metabolites of ethanol degradation whose therapeutic drug monitoring range is between 50 ng/mL and 1000 ng/mL. Its presence in urine can be used to determine recent alcohol intake, even hours after ethanol is no longer detectable. EtG is hydrophilic with a logP value of -1.8. EtG solutions were prepared in *S*urine, which does not contain any endogenous EtG.

The calibration curves for EtG in *S*urine for both polyS-MS and PS-MS were created by plotting EtG concentration versus the EtG:EtG-d5 area ratios. Good linearity of the calibration curve (R^2 = 0.996) was obtained by polyS-MS over the concentration range of 50 ng/mL to 10,000 ng/mL (Table 3). Good reproducibility of the area ratios was achieved at each calibration solution concentration, resulting in very little spread of the replicates as shown for the low concentration range (50-1000 ng/mL) in Fig. 3E. This linearity and low deviation are similar to that for PB in methanol and in *S*urine. The curve's y-intercept is near zero, indicating low background signal as shown (Fig. 3E). In contrast, the data from the PS-MS experiments have poor linearity (R^2 = 0.886) and show very significant spreading of the data with low reproducibility in the lower concentration range (0 ng/mL to 1000 ng/mL) as seen in Fig. 3F. The large y-intercept is indicative of high background signal due to contaminants in the paper sample support. For both polyS-MS and PS-MS, the parent ion (*m/z* 221) was fragmented using a range of collision energies to afford several product ions, including the corresponding $[M\text{-}H]^-$ product ion *m/z* 85 (Table S4). The parent ion of EtG-d5 has an *m/z* 226.

Vancomycin (VAN) in human plasma. VAN, an antibiotic that is used to treat a variety of infections in the body, has a minimum toxic range of 80 μg/mL to 100 μg/mL. It is a highly hydrophilic drug with a logP value of -4.4. Hydrophilic drugs have been shown to be challenging to quantify by PS-MS. OSX polymers have been shown to be very effective in detecting and quantifying very hydrophilic drugs, such as streptomycin (logP -6.4) [13]. Experiments involving a peptide retention time calibration mixture (Table S5) with flat-surface OSX polymers lends further support of the OSX polymers ability to better analyze hydrophilic compounds as compared to paper substrates (Figure S3). Most of the peptides with hydrophobicity factors (HF) below 40 were better analyzed on the OSX polymers with the exception of peptides 3 (HF = 15.52) and 10 (HF = 34.50) as compared to paper over the concentration range of 0 to 5 pM (Figure S3A). Peptide 3 showed high variability in polyS-MS measurements (RSD 70%). Peptides 13, 14, and 15 were better analyzed with PS-MS (Figure S3A). Analysis of the most hydrophobic peptide 15 (HF = 46.66) showed better linearity with the paper substrate (R^2 = 0.980) versus the OSX polymer substrate (R^2 = 0.880) (Figure S3B). In contrast, the analysis of the most hydrophilic peptide (HF = 7.56) showed better linearity with the OSX polymer substrate (R^2 = 0.996) versus the paper substrate (R^2 = 0.961) (Figure S3C).

PolyS-MS and PS-MS analyses of VAN in human plasma were performed along with a comparative polyS-MS analysis using an OSX polymer with a flat surface. The MS data were acquired in positive polarity mode. The parent peak, $[VAN\text{-}HNa]^{2+}$, with *m/z* 735 and the internal standard parent peak, $[VAN\text{-}d12\text{-}HNa]^{2+}$, with *m/z* 742 were observed. The parent peak was fragmented using a range of collision energies to afford several product ions (Table S6). Fig. 3G presents the calibration curve obtained by polyS-MS and plotted as the VAN calibration solution concentrations versus VAN:VAN-d12 area ratios . The calibration curve shows good linearity (R^2 = 0.996) over the full concentration range (80-100 μg/mL, Table 3). The linearity is comparable

Table 4
Peak area ratios and mean recoveries from the analysis of two solutions of PB in *S*urine by polyS-MS, using OSX polymers with surface reservoirs.

PB sample concentration (ng/mL)	*Area Ratio*(PB: PB-d5)	*Mean recovery* (n=3) (%)	*RSD* (%)
250	0.157	90.2	3.51
250	0.165		
250	0.168		
2500	1.29	95.7	2.57
2500	1.23		
2500	1.24		

to the linearities obtained for PB in methanol and EtG in urine by polyS-MS (Table 3). In the case of human plasma, *in situ* protein precipitation was performed on the polymer surface prior to analysis by directly depositing a small volume of methanol on the VAN-spiked plasma before drying (Figure S4) to partially release VAN from the proteins in plasma. Three different approaches for protein precipitation by addition of methanol were tested: (1) offline plasma precipitation, (2) precipitation of dried sample spot on OSX polymer, and (3) precipitation of wet sample spot (before drying) on OSX polymer. In all three cases, the absolute areas were similar (Table S7), but precipitation of proteins from a wet sample was much more successful than from a dried sample spot, which required rewetting with a larger volume of solvent than for the wet sample spot case (Table S7).

VAN was also analyzed by polyS-MS, using OSX polymers with flat surfaces. The corresponding calibration curve had moderate linearity ($R^2 = 0.973$) with a y-intercept of -0.9 over the concentration range of 5 μg/mL to 50 μg/mL (Figure S5). The lack of signal at lower concentrations of VAN on a flat polymer could be a result of dilution of the analyte by the solvent. VAN was not detected by PS-MS at any concentration we investigated.

3.3. Quantitative analysis of PB quality control samples

Two PB concentrations in *S*urine, 250 ng/mL and 2500 ng/mL, were analyzed by polyS-MS, using OSX polymers with surface reservoirs to hold the spray solvent. Good reproducibility of peak areas and area ratios were obtained as shown in Table 4. Better recovery was achieved at the higher PB sample concentration. The mean recoveries of 250 ng/mL PB sample (n=3) and 2500 ng/mL PB sample (n=3) were 90.2% (RSD 3.51%) and 95.7% (RSD 2.57%), respectively.

3.4. Effect of polymer morphology on signal stability and intensity

The stability of the signals generated by the mass spectrometer using an OSX polymer sample support with and without a surface reservoir (i.e., flat surface) was analyzed using PB in *S*urine. Fig. 4A and B show two graphs of the detected signal (relative abundance) as a function of time generated during polyS-MS analysis using an OSX polymer with a surface reservoir and an OSX polymer with a flat surface, respectively.

The OSX polymer with a surface reservoir has several advantages over OSX polymer with a flat surface. First, with the same amount of solvent, a polymer with a surface reservoir yielded a stable signal with a longer duration (> 2 min) than a polymer with a flat surface. A lower volume of spray solvent (~40 μL) was used with the OSX polymer with surface reservoir as compared to the OSX polymer with a flat surface, which required more than 40 μL to maintain a steady spray and introduce ions into the mass spectrometer. Second, the observed area ratio % RSD was improved (<5%) for a 1000 ng/mL PB sample analyzed with a polymer with a surface reservoir compared to a flat surface. Third, the OSX polymer with surface reservoir was easier and faster to align with the mass spectrometer inlet than the flat surface polymer. A spray would consistently form from the upper edge of the triangular tip. Alignment of the OSX polymer with a flat surface to the mass spectrometer inlet in a position that allows solvent to steadily reach the tip and be ionized was difficult to achieve. Some flat polymers could not produce an ion signal.

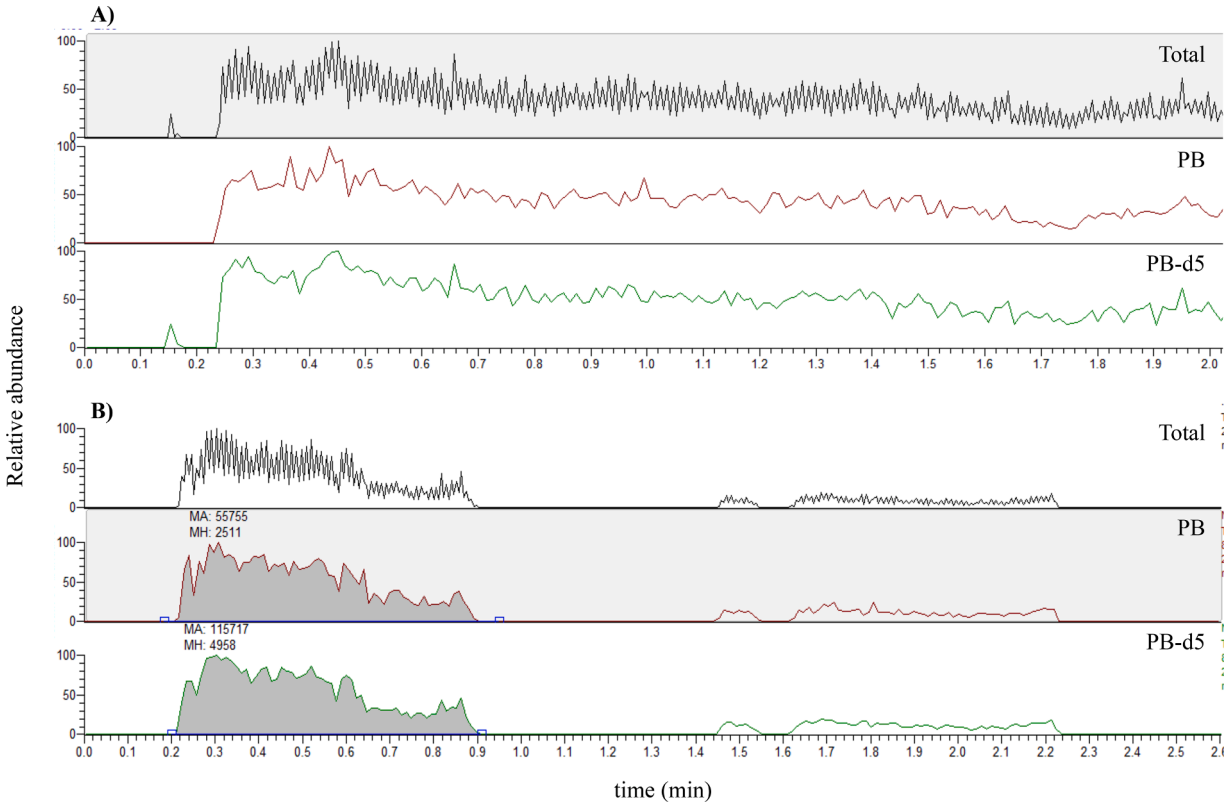

Fig. 4. Signal stability of PB in *S*urine analysed by polyS-MS, using OSX polymer with (A) a surface reservoir and (B) a flat surface.

Fourth, the hydrophobic nature of the OSX polymers means that the spray solvent sits on the surface; a large droplet can reach the tip of a flat polymer and cause a discharge. Discharging was not a problem with the OSX polymers with surface reservoirs.

Similarly, longer signal duration and stability were achieved for EtG in *S*urine (1000 ng/mL) and VAN in human plasma (100 μg/mL) as compared to paper, as shown in Figures S6 and S7, respectively. The EtG signal using the OSX polymer with surface reservoir lasted for approx. 2.5 min with 40 μL of spray solvent while with paper the signal lasted for only 1 min for the same spray solvent volume (Figure S6A). When another 20 μL of spray solvent was added to the paper, the signal intensity once again reached a maximum for only about 0.3 min (Figure S6B). The VAN signal using an OSX polymer with a surface reservoir lasted for about 3 min with 40 μL of spray solvent (Figure S7).

Signal intensities for the fragment ions *m/z* 75 and 85 for EtG in methanol analyzed by polyS-MS using a flat-surface OSX polymer were 2 orders of magnitude larger than for paper (see Table S8). A signal intensity of 7.78×10^3 was obtained for *m/z* 75 and 7.64×10^3 for *m/z* 85 by polyS-MS analysis. In contrast, when paper was used, the signal intensity of fragment ion *m/z* 75 was 2.24×10 and 1.93×10 for *m/z* 85. To maintain sufficient signal, 3 times the volume of spray solvent was needed for PS-MS (60 μL) as compared to polyS-MS (20 μL). The fragment peaks are identified in the mass spectrum of EtG in methanol (polyS-MS) as shown in Figure S8.

4. Conclusion

We have shown that an OSX polymer with a surface reservoir to contain the spray solvent enhances the signal stability of hydrophilic drug samples during analysis by polyS-MS. When compared to paper, OSX polymer substrates allow for the quantitative analysis of hydrophilic drugs at low concentrations that are not easily detectable with paper-spray MS. Using OSX polymer substrates with surface reservoirs, calibration curves were generated with good linearity and low data spread over the concentration ranges used for each of the drugs tested. The ability to tailor the morphology of OSX polymers allows for a wider range of polymers to further develop polyS-MS and broaden the scope of its application to drug and disease surveillance.

Declaration of Competing Interest

The authors declare that they have no known competing financial interests.

Author contributions

Maria T. Dulay: Conceptualization, Investigation, Data curation, Writing – review & editing **Cornelia L. Boeser:** Investigation, Data curation, Writing – review & editing. **Katherine L. Walker:** Investigation, Data curation, Writing – review & editing. **Clara Feider:** Investigation, Writing – review & editing. **Richard N. Zare:** Conceptualization, Writing – review & editing, Supervision.

Acknowledgments

This work was supported by Thermo Fisher Scientific [Stanford Grant #131701] and by the Chief Scientist's Office of Thermo Fisher Scientific. We thank Harikrishnan Sukumar for his assistance in design and 3D printing of the molds.

Supplementary materials

Supplementary material associated with this article can be found, in the online version, at doi:10.1016/j.talo.2021.100048.

References

[1] W. Clark, Therapeutic drug monitoring, in: W. Clarke, M.A. Marzinke (Eds.), Contemporary Practice in Clinical Chemistry, Academic Press, London, 2020, pp. 905-915. 10.1016/B978-0-12-815499-1.00051-X.
[2] N. Stephanson, H. Dahl, A. Helander, O. Beck, Direct quantification of ethyl glucuronide in clinical urine samples by liquid chromatography-mass spectrometry, Ther. Drug Monitoring 24 (2002) 645–651.
[3] K. Freudenberger, U. Hilbig, Gauglitz, Recent advances in therapeutic drug monitoring of immunosuppressive drugs, Trends in Anal. Chem. 79 (2016) 257–268.
[4] A. Dasgupta, M.D. Krasowski, Application of chromatographic techniques for therapeutic drug monitoring, in: A. Dasgupta, M.D. Krasowski (Eds.), Therapeutic Drug Monitoring Data: A Concise Guide, Academic Press, London, 2020, pp. 53–63, https://doi.org/10.1016/B978-0-12-815849-4.00005-0.
[5] E.M. McBride, P.M. Mach, E.S. Dhummakupt, S. Dowling, D.O. Carmany, P. S. Demond, G. Rizzo, N.E. Manicke, T. Glaros, Paper spray ionization: applications and perspectives, Trends Anal. Chem. 118 (2019) 722–730.
[6] Q. Yang, H. Wang, D.J. Maa, J.W. Chappell, N.E. Manicke, R.G. Cooks, Z. Ouyang, Paper spray ionization devices for direct, biomedical analysis using mass spectrometry, Int. J. Mass Spectrom. 312 (2012) 201–207.
[7] Y. Su, J. Wang, J. Liu, P. Wei, R.G. Cooks, Z. Ouyang, Quantitative paper spray mass spectrometry analysis of drugs of abuse, Analyst 138 (2013) 4443–4447.
[8] N.E. Manicke, P. Abu-Rabie, N. Spooner, Z. Ouyang, R.G. Cooks, Quantitative analysis of therapeutic drugs in dried blood spot samples by paper spray mass spectrometry: an avenue to therapeutic drug monitoring, J. Am. Soc. Mass Spectrom. 22 (2011) 1501–1507.
[9] S. D'Aronco, M. Dall'Armi, S. Crotti, E. Calandra, P. Traldi, V. Di Marco, A. Buonadonna, G. Corona, L. Giodini, E. Marangon, B. Posocco, G. Toffoli, M. Agostini, Field-assisted paper spray mass spectrometry for therapeutic drug monitoring: 1. The case of imatinib in plasma, J. Mass Spectrom. 52 (2017) 283–289.
[10] R.D. Espy, N.E. Manicke, Z. Ouyang, R.G. Cooks, Rapid analysis of whole blood by paper spray mass spectrometry for point-of-care therapeutic drug monitoring, Analyst 137 (2012) 2344–2349.
[11] L. Shen, J. Zhang, Q. Yang, N.E. Manicke, Z. Ouyang, High throughput paper spray mass spectrometry analysis, Clin. Chim. Acta 420 (2013) 28–33.
[12] J. McKenna, R. Jett, K. Shanks, N.E. Manicke, Toxicological drug screening using paper spray high-resolution tandem mass spectrometry (HR-MS/MS), J. Anal. Toxicol. 42 (2018) 300–310.
[13] M.T. Dulay, R.N. Zare, Polymer-spray mass spectrometric detection and quantitation of hydrophilic compounds and some narcotics, Rap. Commun. Mass Spec. 31 (2017) 1651–1658.
[14] P.W. Fedick, B.J. Bills, N.E. Manicke, R.G. Cooks, Forensic sampling and analysis from a single substrate: surface-enhanced Raman spectroscopy followed by paper spray mass spectrometry, Anal. Chem. 89 (2017) 10973–10979.
[15] S.F.P. Da, E.S.D. Da Fernandes, R. Augusti, E. Piccin, Forensic analysis of ballpoint pen inks using paper spray mass spectrometry, Analyst 140 (2015) 811–819.
[16] H. Wang, Y. Ren, M.N. McLuckey MN, N.E. Manicke, J. Parkk, L. Zheng, R. Shi, R. G. Cooks, Z. Ouyang, Direct quantitative analysis of nicotine alkaloids from biofluid samples using paper spray mass spectrometry, Anal. Chem. 85 (2013) 11540–11544.
[17] J. Ji, L. Nie, L. Liao, R. Du, B. Liu, P. Yang, Ambient ionization based on mesoporous graphene coated paper for therapeutic drug monitoring, J. Chromatogr. B 1015-1016 (2016) 142–149.
[18] D.E. Damon, K.M. Davis, C.R. Moreira, P. Caponne, R. Cruttenden, A.K. Badu-Tawiah, Direct biofluid analysis using hydrophobic paper spray mass spectrometry, Anal. Chem. 88 (2016) 1878–1884.
[19] D.E. Damon, Y.S. Maher, M. Yin, F.P.M. Jjunju, I.S. Young, S. Taylor, S. Maher, A. K. Badu-Tawiah, 2D wax-printed paper substrates with extended solvent supply capabilities allow enhanced ion signal in paper spray ionization, Analyst 141 (2016) 3866–3873.
[20] W. Han, Y. Zheng, T. Muyizere, Z. Zhang, Development of paper substrate for paper spray MS in high-sensitivity analysis of biological samples, Bioanalysis 10 (2018) 2047–2067.
[21] Q. Wang, Y. Zheng, X. Zhang, X. Han, T. Wang, Z. Zhang, A silica coated paper substrate: development and its application in paper spray mass spectrometry for rapid analysis of pesticides in milk, Analyst 140 (2015) 8048–8056.
[22] T.C. Colletes, P.T. Garrcia, R.B. Campanha, P.VV. Abdelnnur, W. Romão, W.K. T. Coltro, B.G. Vaz, A new insert sample approach to paper spray mass spectrometry: a paper substrate with paraffin barriers, Analyst 141 (2016) 1707–1713.
[23] X. Zhang, S. Xu, J.M. Lim, Y.I. Lee, Molecularly imprinted solid phase microextraction fiber for trace analysis of catecholamines in urine and serum samples by capillary electrophoresis, Talanta 99 (2012) 270–276.
[24] T.P.P. Mendes, I. Pereira, M.R. Ferreira, A.R. Chaves, B.G. Vaz, Molecularly imprinted polymer-coated paper as a substrate for highly sensitive analysis using paper spray mass spectrometry: quantification of metabolites in urine, Anal. Methods 9 (2017) 6117–6123.
[25] T. Want, Y. Zheng, X. Wang, D.E. Austin, Z. Zhang, Sub-ppt mass spectrometric detection of therapeutic drugs in complex biological matrices using polystyrene-microsphere-coated paper spray, Anal. Chem. 89 (2017) 7988–7995.
[26] J. Li, Y. Zheng, W. Mi, T. Muyizere, Z. Zhang, Polystyrene-impregnated paper substrates for direct mass spectrometric analysis of proteins and peptides in complex matrices, Anal. Methods 10 (2018) 2803–2811.

[27] Y. Ren, H. Wang, J. Liu, Z. Zhang, M.N. McLuckey, Z. Ouyang, Analysis of biological samples using paper spray mass spectrometry: an investigation of impacts by the substrates, solvents and elution methods, Chromatographia 76 (2013) 1339–1346.
[28] G.I. Salentijn, H.P. Permentier, E. Verpoorte, 3D-Printed paper spray ionization cartridge with fast wetting and continuous solvent supply features, Anal. Chem. 86 (2014) 11657–11665.
[29] H. Lee, C.S. Jhang, J.T. Liu, C.H. Lin, Rapid screening and determination of designer drugs in saliva by a nib-assisted paper spray-mass spectrometry and separation technique, J. Sep. Sci. 35 (2012) 2822–2825.
[30] W. Sun, F.Q. Yang, Evaporation-assisted formation of surface patterns from polymer solutions *via* copper tubes, eXPRESS Polym. Lett. 12 (2018) 699–712.
[31] K.Z. Donato, L. Matejka, R.S. Mauler, R.K. Donato, Recent applications of ionic liquids in the sol-gel process for polymer-silica nanocomposites with ionic interfaces, Coll. Interf. 1 (2018) 5.
[32] S.J. Kang, V. Vandadi, J.D. Felske, H. Masoud, Alternative mechanism for coffee-ring deposition based on active role of free surface, Phys. Rev. E. 94 (2016), 063104.
[33] Drugbank. https://www.drugbank.ca, 2020 (accessed December 20, 2020).
[34] N. Riboni, A. Quaranta, H.V. Motwani, N. Österlund, A. Gräslund, F. Bianchi, L. L. Ilag, Solvent-assisted paper spray ionization mass spectrometry (SAPSI-MS) for the analysis of biomolecules and biofluids, Sci. Rep. 9 (2019) 10296.
[35] G.I. Salentijn, H.P. Permentier, E. Verpoorte, 3D-printed paper spray ionization cartridge with fast wetting and continuous solvent supply features, Anal. Chem. 86 (2014) 11657–11665.
[36] S. Dai, Y.H. Ju, H.J. Gao, J.S. Lin, S.J. Pennycook, C.E. Barnes, Preparation of silica aerogel using ionic liquids as solvents, Chem. Commun. 3 (2000) 243–244.
[37] L. Viau, M.A. Néouze, C. Biolley, S. Volland, D. Brevet, P. Gaveau, P. Dieudonné, A. Galarneau, A. Vioux, Ionic liquid mediated sol-gel synthesis in the presence of water or formic acid: which synthesis for which material, Chem. Mater. 24 (2012) 3128–3134.
[38] L.Viau A.Vioux, S. Volland, J. Le Bideau, Use of ionic liquids in sol-gel; ionogels and applications, C. R. Chimie 13 (2010) 242–255.
[39] A. Karim, T.M. Slawecki, S.K. Kumar, J.F. Douglas, S.K. Satija, C.C. Han, T. P. Russell, Y. Liu, R. Overney, J. Sokolov, M.H. Rafailovich, Phase-separation-induced surface patterns in thin polymer blend films, Macromolecules 31 (1998) 857–862.
[40] M. Yamamura, T. Nishio, T. Kajiwara, K. Adachi, Evaporation-induced pattern formation in polymer films via secondary phase separation, Chem. Eng. Sci. 57 (2002) 2901–2905.
[41] Z. Mitov, E. Kumacheva, Convection-induced patterns in phase-separating polymeric fluids, Phys. Rev. Lett. 81 (1998) 3427–3430.
[42] T.H. Choi, S.M. Do, B.G. Jeon, S.T. Shin, T.H. Yoon, Formation of polymer walls through the phase separation of a liquid crystal mixture induced by a spatial elastic energy difference, Sci. Rep. 9 (2019) 10288.
[43] K. Nakanishi, N. Tanaka, Sol-gel with phase separation. Hierarchically porous materials optimized for high-performance liquid chromatography separations, Acc. Chem. Res. 40 (2007) 863–873.
[44] Y. Tan, W. He, S. Wang, Z. Tao, L. Cheng, The superiority of silver nanoellipsoids synthesized via a new approach in suppressing the coffee-ring effect during drying and film formation processes, Nanotech 25 (2014), 125602.
[45] G. Li, K. Graf, E. Bonnaccuros, D.S. Golovko, A. Best, H.J. Butt, Evaporation structures of solvent drops evaporating from polymer surfaces: influence of molar mass, Macromol. Chem. Phys. 208 (2007) 2134–2144.
[46] H. Yang, M. Su, K. Li, L. Jiang, Y. Song, M. Doi, J. Wang, Preparation of patterned ultrathin polymer films, Langmuir 30 (2014) 9436–9441.
[47] S. Rivera-Rubero, S. Baldelli, Influence of water on the surface of hydrophilic and hydrophobic room-temperature ionic liquids, J. Am. Chem. Soc. 126 (2004) 11788–11789.